



BUILDING RETROFIT PRIOR TO DAMAGING EARTHQUAKES: REDUCTION OF RESIDUAL CAPACITY AND REPAIR COSTS

M. Gaetani d'Aragona⁽¹⁾, M. Polese⁽²⁾, M. Di Ludovico⁽³⁾

⁽¹⁾ Research fellow, University of Naples Federico II, marco.gaetanidaragona@unina.it

⁽²⁾ Assistant Professor, University of Naples Federico II, mapolese@unina.it

⁽³⁾ Assistant Professor, University of Naples Federico II, diludovi@unina.it

Abstract

When a seismic event occurs, damage may accumulate in a building affecting its capacity to withstand future earthquakes. This study investigates, by means of a detailed case study, the advantages related to the application of structural retrofit prior of earthquake events in terms of structural safety variation due to damage. The response of an existing non-ductile RC frame in California is simulated using a refined finite element model that properly accounts for possible brittle failures of structural members. Furthermore, the actual structural capacity is evaluated accounting for typical collapse modes that can affect the behavior of non-ductile buildings. Different retrofit strategies have been adopted and damaging earthquake scenarios considered. The future seismic performances of retrofitted structure before damage are compared with the case in which no mitigation strategies have been adopted showing the advantages of different categories of intervention for different earthquake scenarios.

Keywords: Retrofit, Residual Capacity, Repair costs.



1. Introduction

Reinforced concrete buildings designed and constructed prior to the introduction of principles of capacity design represents the largest building stock in all over the world. For these structures, strong earthquakes can result in severe damage or collapse, posing a significant threat to life of occupants and leading to loss of critical building content and functionality [1] (i.e., direct losses). In addition, after earthquakes, many buildings may be closed pending determination of safety and necessary repairs and strengthening [2] for long periods significantly protracting recovery phase (i.e., indirect losses). Increasing the resilience of physical system may significantly reduce the exposure of life and properties as well as recovery time. This target can be pursued by promulgating active code provisions that reduce community risk by requiring seismic upgrading of particularly vulnerable buildings, guiding through the prioritization of retrofit applications and the selection of optimal mitigation strategy.

Generally, for single buildings the selection of a particular retrofitting technique is guided by the ratio between seismic demand and capacity, target performance level, difficulties of intervention as well economic constraints imposed by owners. The optimal retrofit strategy can be then determined through iterative analysis of the structure for various retrofit strategies. In particular, for structures at or close to the life-safety performance level, the risk of collapse is relatively low, and thus, risk assessment and loss estimation study can be performed for such structures to make a retrofit decision based on potential level of losses. However, when structures are non-conforming to present seismic provisions, additional metrics should be considered to lead the choice of the optimal retrofit strategy. In fact, even if a non-ductile building does not result in partial or complete collapse, the structural damage experienced during a major earthquake may cause a significant seismic safety decay, critically reducing building's future seismic performances [3]. Mitigation strategies applied during peacetime can reduce damage and economic losses as well as avoid a critical performance loss, making the building eligible for repair actions after damage.

For these reasons, the selection of optimal retrofit intervention, along with the reduction of seismic hazard, should account for future seismic performances both in terms of reduction of repair costs and decay of seismic capacity after damage to make the building more resilient, and so significantly shortening the recovery phase.

This is particularly important when there is a need to apply mitigation strategies for reducing seismic hazard for a large structural inventory, at regional scale, when the major scope is to guarantee safety respecting multiple constraint strictly relate to both direct and indirect losses. The main research challenge remains in fact, the seismic evaluation and prioritization of structures maximizing the accuracy and the reliability of procedure using methodologies as simple as possible. In order to achieve this, there is a need to perform pilot studies that involve both approximate and detailed evaluation of structures to gain insight into the performance of approximate methods and their correlation with the detailed procedures.

In this study we address the advantages related to the application of structural retrofit prior of earthquake events both in terms of structural safety variation due to damage and in terms of direct losses. The response of an existing non-ductile RC frame is simulated using a refined finite element model that properly accounts for possible brittle failures of structural members. Two different retrofit strategies have been adopted and two different damaging earthquake scenarios considered. The future seismic performances of retrofitted structure before damage are compared with the case in which no mitigation strategies have been adopted showing the advantages and the effectiveness of different categories of intervention for different earthquake scenarios.

2. T_R -dependent aftershock fragilities

The building capacity after a damaging earthquake may be significantly reduced due to the spread of damage all over the building, while the probability of collapse increases. Seismic behavior of damaged buildings, and their relative seismic safety, may be suitably represented by their seismic capacity modified due to damage, the so-called RESidual Capacity (REC) [4], which can be expressed in terms of collapse fragility curves after damage. In this study Aftershock (AS) fragility curves are derived depending on the intensity of the damaging earthquake, Mainshock (MS), corresponding to T_R in a given hazard area.

2.1 Damage scenarios and ground motion selection

Two different earthquake scenarios, corresponding to 72 and 475 years return periods are considered, corresponding to probabilities of exceeding of 50% and 10% in 50 years, respectively. A set of 31 ground motions is selected from the PEER Next Generation Attenuation (NGA) database [5]. Ground motions MS-AS sequences are generated using this ground motions set where single earthquakes are applied as both MSs and ASs. For further information on selection of accelerograms, refer to [6].

2.2 Collapse criteria

Older RC structures, non-conforming to modern design standards, are likely to experience gravity load collapse prior to side-sway collapse [7]. For this reason, this study considers two possible collapse mechanisms to capture the actual capacity in the non-ductile model, as firstly proposed in [6]: Side-sway collapse (SC) and Gravity load collapse (GLC). The SC occurs when a single storey has reached its capacity to withstand lateral loads (i.e., when every column in a given floor has exceeded its residual shear capacity at the same time). GLC occurs when vertical load demand exceeds the total vertical load capacity at a given storey. Collapse is detected based on a comparison of storey-level gravity load demands and capacities (adjusted at each time step to account for member damage and load redistribution). The gravity load demand is considered constant during each analysis. An additional collapse criterion is considered when Carbon Fibre Reinforced Polymer (CFRP) wrapping is applied to all columns in a storey: the collapse is attained when a small increase in ground-shaking intensity causes a large increase in lateral drift response, i.e. instability collapse (IC), or when interstorey drift ratio exceeds the 10% threshold.

An internal algorithm monitors the dynamically varying capacity of each element and checks the GLC and SSC criteria throughout each nonlinear time history analysis to detect the collapse. A bisection algorithm is then implemented to find the collapse capacity with a precision of 0.05g during the IDA procedure. The collapse is considered as the first between GLC, SSC, and IC for floors in which CFRP wrapping is applied.

2.3 Derivation of Mainshock and T_R -dependent Aftershock fragilities

The fragility computation is based on the use of IDA analyses [8], scaled up until collapse is reached; $S_a(T_1)$ is assumed as intensity measure (IM) for the earthquake shaking.

To quantify structural response of the intact building, IDA is carried out on the nonlinear model of undamaged building using the set of 31 ground motions acting as MS. REC for each MS is calculated as the spectral intensity corresponding to the attainment of structural collapse.

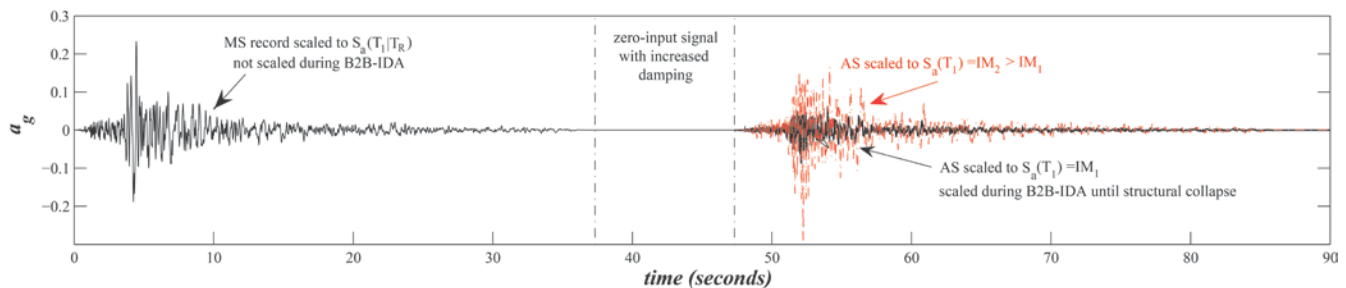


Fig. 1 – Example of MS-AS sequence for B2B-IDA

In order to evaluate AS fragilities, multiple earthquake sequences MS-AS are built through suitable scaling of selected accelerograms (see Fig. 1). In particular, the MS record is scaled to represent different Return Periods for the specific area and structure. For each (scaled) MS nonlinear time history is performed and the response is recorded; then an AS record is applied to the MS-damaged structure. A time gap of 10 seconds between MS and AS, with increased critical damping, is considered to allow the ceasing of vibration produced by the MS. Dynamic AS analysis is repeated with increasing scale factor applied to the AS record, providing IDA analysis results for MS-damaged structure, until the MS-AS sequence causes collapse. To account for the effect of record-to-record



variability on structural response MS-AS sequences are generated using the entire set of 31 ground motions that are applied as both MSs and ASs, generating a total of 961 record sequences for each return period.

The capacity of MS-damaged building is computed in terms of S_a based on the IDA results obtained from MS-AS sequences. The results are here represented in terms of fragility curve at collapse. For the undamaged building, the collapse fragility curve is based on the IDA results performed on the intact building using the set of 31 ground motions. The collapse fragility curve for damaged building is calculated based on the AS collapse capacities obtained for each of 961 MS-AS sequences in which the MS is scaled in order to be representative of the T_R of interest.

2.4 Analytical formulation for T_R -dependent aftershock fragilities

Starting from the initial damage state produced by a MS corresponding to a given T_R , T_R -dependent collapse fragility functions can be built. Because the structure is subject to a series of consecutive events, cumulative damage is accounted for in the estimate of the collapse probability.

Considering a seismic sequence consisted of a pair of MS and the consecutive aftershock event AS, the aftershock collapse probability conditioned on the MS intensity, $S_{a,MS}$, can be calculated by considering two mutually exclusive and collectively exhaustive events [9] defined as C and NC (Eq. (1)). C accounts for cases where collapse occurs due to the mainshock and NC accounts for cases where collapse does not take place due to the MS [10,11]. In Eq. (1) $S_{a,MS}$ is MS spectral acceleration corresponding to a specific T_R conditioned on the site hazard, the fundamental vibration period of the intact structure (T_1), and the critical damping ratio assumed; $S_{a,AS}$ is the AS spectral intensity at T_1 and $S_{a,AS}^C$ is the AS spectral intensity corresponding to collapse. Assuming an equal probability of occurrence for each MS, the term $P(NC/S_{a,MS})$ can be estimated as the number of NC-cases over the number of MS considered (N_{MS}), while $P(C/S_{a,MS})$ can be estimated as the number of C-cases over N_{MS} and $P(x \geq S_{a,AS}^C / S_{a,MS}, C) = 1$. Hence, the AS fragility can be interpreted, for each considered structure and T_R (corresponding to $S_{a,MS}$), as the sum of the MS collapse fragility (last term in Eq. (1)), and an inflating term (first term in Eq. (1)). $P(x \geq S_{a,AS}^C / S_{a,MS}, NC)$ is the collapse probability conditioned on MS intensity $S_{a,MS}$ and on NC and can be expanded as in Eq. (2). Eq. (2) \underline{MS} stands for the MS wave-form vector; $f(\underline{MS} / S_{a,MS}, NC)$ is the joint probability density function for the MS wave-form vector given a specific value for $S_{a,AS}$ and given NC.

$$P(x \geq S_{a,AS}^C | S_{a,MS}) = P(x \geq S_{a,AS}^C | S_{a,MS}, NC) \cdot P(NC | S_{a,MS}) + P(x \geq S_{a,AS}^C | S_{a,MS}, C) \cdot P(C | S_{a,MS}) \quad (1)$$

$$P(x \geq S_{a,AS}^C | S_{a,MS}, NC) = \int_{\forall \underline{MS}} P(x \geq S_{a,AS}^C | \underline{MS}, S_{a,MS}, NC) \cdot f(\underline{MS} | S_{a,MS}, NC) dMS \approx \frac{1}{N_{NC}} \sum_{i=1}^{N_{NC}} P(x \geq S_{a,AS}^C | \underline{MS}_i, S_{a,MS}, NC) \quad (2)$$

The integral in Eq. (2) is an application of the Total Probability Theorem in conditioning on all possible \underline{MS} waveforms conditioned on a given S_a value. It should be noted that the approximation to the integral in Eq. (2) is based on the assumption that the various MS wave-forms have equal probability of occurrence [12].

3. Economic Loss analysis

Direct costs associated to repair and/or substitution of the building due to both structural and non-structural damage due to earthquakes are generally considered as additional metrics of building seismic performance. This metric can support stakeholders' decisions with information, usually in probabilistic terms, about the risk for the building in terms of earthquake economic losses, which is a means of quantifying and communicating risk.

To evaluate expected economic losses for the studied building, the performance-based framework established by the Pacific Earthquake Engineering Research Center (PEER) is adopted [13]. The PEER methodology consists of four subsequent steps: hazard analysis, structural response analysis, evaluation of damage and economic loss analysis. The outcome of each analysis is then integrated using the Total Probability Theorem, allowing to take into account combined numerical integration of all the conditional probabilities and to propagate the uncertainties from one level of analysis to the next, resulting in probabilistic prediction of performance.

In this study, the same ground motion bin adopted to carry out T_R -dependent aftershock fragility curves is been used to perform response analysis structural model of the facility. The response in terms of engineering demand parameters (EDPs), such as peak interstorey drift and peak floor acceleration, conditioned on the intensity measure, is carried out for each considered model and level of the seismic action considered adopting nonlinear response-history analyses. The damage analysis adopts a collection of damage fragility functions and unit repair-cost distribution functions for damageable building components as proposed in [14]. Fragility functions for both drift and acceleration-sensitive components are used, uncertainty in repair costs is neglected and the expected value of component repair cost expressed as a fraction of component cost as new is adopted. Architectural layouts, components and cost of new elements were adopted from [15]; those data are necessary for effective quantification of the amount of damage and costs in the real building. More details can be found in Gaetani d’Aragona [16, 17]. Only direct monetary losses (i.e., repair costs) were considered. Further details on the adopted procedure can be found elsewhere (e.g., [18,19]).

4. Application to a Non-Ductile Building

The building selected for this study is the perimeter moment resisting frame of the Van Nuys Holiday Inn, that is a seven-story eight-bay non-ductile reinforced concrete frame building located in Los Angeles, California.

4.1 Original non-ductile building

A two-dimensional finite element MDOF model developed using OpenSees [20] is adopted to simulate the seismic response of the building. Beams and columns are modelled using the nonlinear beam-column element [21].

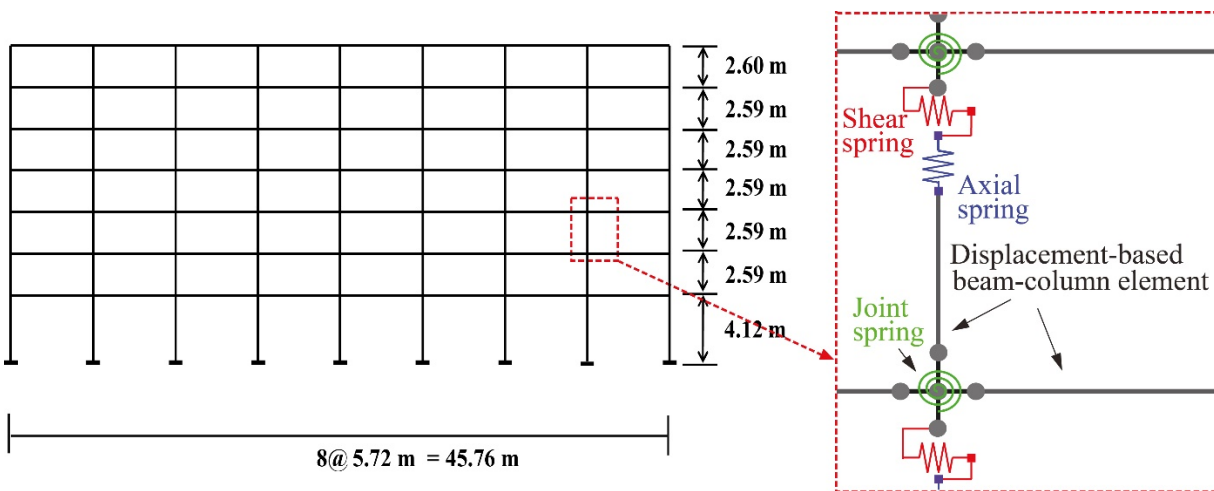


Fig. 2 – South frame elevation and column, beam and joint models.

Due to non-ductile details that characterize both of the structures, is expected that the joints may influence the failure mechanism, consequently the joints are modeled using rotational spring elements, the so-called “scissor model” [22], including a pinching hysteric behavior to account for the nonlinear shear deformation of the joint. Similarly, shear and axial failure are expected to occur in non-ductile detailed columns, and consequently shear and axial failure in the columns are modeled using the Limit State material [23]. Bond-slip rotations for beams have been included modifying joint backbone as proposed in [24]. P- Δ effects are included. A schematic view of the adopted numerical model is shown in Fig. 2.

The eigenvalue analysis of the intact structure provides a fundamental vibration period of 1.0 sec. A damping of 2% is assigned to the first and third modes using Rayleigh damping. The damping is updated during the first-to-second earthquake analysis at the beginning of each seismic sequence, accounting for the first mode period elongation due to structural damage.

4.2 CFRP-wrapped building

The retrofit strategy consists in the application of CFRP layers to enhance the structural performance of RC columns. The wrapping is applied to all columns of selected storeys and columns are fully wrapped for their entire height to provide an efficient confinement effect. Column wrapping was designed in order to prevent columns shear failure after yielding. In particular, the ACI 369R-11[25] was adopted in the design process in order to provide a shear resistance such that flexural failure was ensured [26].

Two different wrapping configurations were adopted to represent localized and widespread interventions: in the first configuration (*wrap1*, Fig.3a) columns at storeys 1st and 7th are fully wrapped, while in the second (*wrap2*, Fig.3b) columns at storeys 1st- and from 4th- to 7th. Intervention *wrap1* is designed considering shear failure occurred during the MSs for the original structure, while intervention *wrap2* is designed to avoid brittle failures occurred during the MSs for the model *wrap1*. For both models, when the wrapping is applied to columns, brittle failure is avoided for all storey columns and their behavior is modeled considering only flexural behavior. The modified behavior of columns materials, due to confining action applied by the CFRP wrapping, is accounted for implementing stress-strain relationship proposed by Spoelstra and Monti [27].

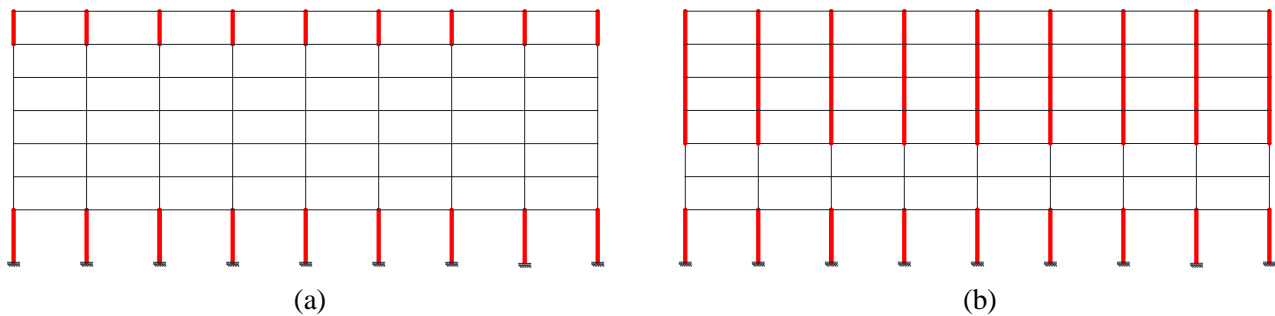


Fig. 3 – Retrofit strategies: (a) *wrap1* - CFRP wrapping at 1st and 7th storey; (b) *wrap2* - CFRP wrapping at 1st and from 4th to 7th storey.

5. Results

5.1 Mainshock fragility curves

For the undamaged building, the collapse fragility curve is based on the IDA results performed on the intact building using the selected set of 31 ground motions.

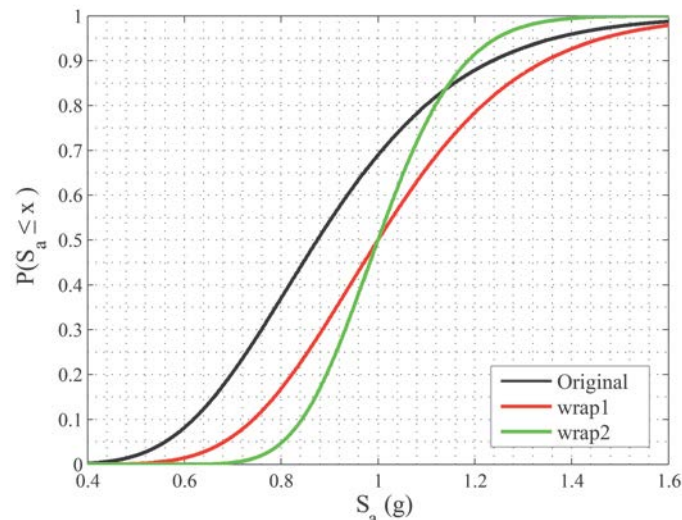


Fig. 4 – MS fragility curve for studied models.



Fig.4 depicts the collapse fragility curves for the original building (black line), for models *wrap1* (red), and *wrap2* (green). It can be observed the original fragility curve shifts right when retrofit is applied, leading to an increase of collapse capacity for the intact building of about 14%. However, it is clear that despite the application of a widespread wrapping, *wrap2* does not lead to an increase of median collapse capacity with respect to *wrap1*. This effect can be explained considering that the most of collapses for *wrap1* occurs at 1st storey, and for those cases, additional wrappings considered in scheme *wrap2* are ineffective. Only for some records CFRP wrapping is efficient, generally leading to a concentration of collapses in the 1st storey, and thus relatively reducing collapse capacity dispersion.

5.2 T_R -dependent fragility curves

The collapse fragility curve for damaged building is calculated based on the aftershock collapse capacities obtained for each of 961 MS-AS sequences in which the MS is scaled in order to be representative of the T_R of interest. Fig. 5 illustrates the collapse fragility curves for the intact and damaged building in terms of probability of collapse conditioned on the MS for given T_R , as a function of AS spectral intensity, $S_{a,AS}(T_1)$. The continuous line represents the behavior of the intact building. As the T_R increases, due to the increasing building damage for MS application, the collapse fragility curve shift left and up. Because for increasing T_R an increasing number of collapses due to MS is detected, the collapse fragility curves for higher T_R have nonzero probability of collapse for $S_{a,AS}=0$.

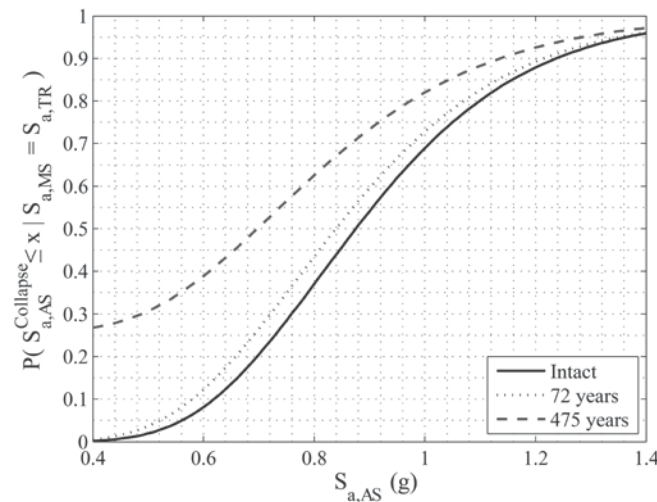


Fig. 5 – T_R -dependent fragility curves and fragility curve for the original building (see [3, 15])

Figs. 6 and 7 show the aftershock fragility curves for the retrofitted building with scheme *wrap1* and *wrap2*, respectively. For comparison purpose, the aftershock fragility curves obtained for the non-retrofitted building is reported on the same graph in light gray. Similarly, to what obtained for the original model, when CFRP wrapping is applied to 1st and 7th storeys, the damage produced by MSs reduces aftershock collapse capacity as the intensity of the ground motion increases (Fig.6). However, while for $T_R=72$ yrs the variation of capacity (i.e., the distance between MS and AS fragility curves) is similar to that obtained for the original non-ductile model, also having a similar dispersion, when the building is subjected to 475 yrs earthquakes, the wrapping scheme leads to a reduced variation of capacity and to a higher aftershock capacity. Note that despite the curve for 475 yrs also have non-zero probability of collapse for $S_{a,AS}=0$, the median collapse capacity is higher with respect to that for the original model because of the reduced number of records causing collapse during MS.

Fig. 7 shows the aftershock fragility curves obtained for the retrofitted building with scheme *wrap2*. The aftershock fragility curve shows that median collapse capacity of damaged building does not decrease with respect to that obtained for the intact structure. In fact, despite the MS fragility leads to the same median capacity, shown in Fig.4, the aftershock capacity results to be influenced by the different wrapping scheme.

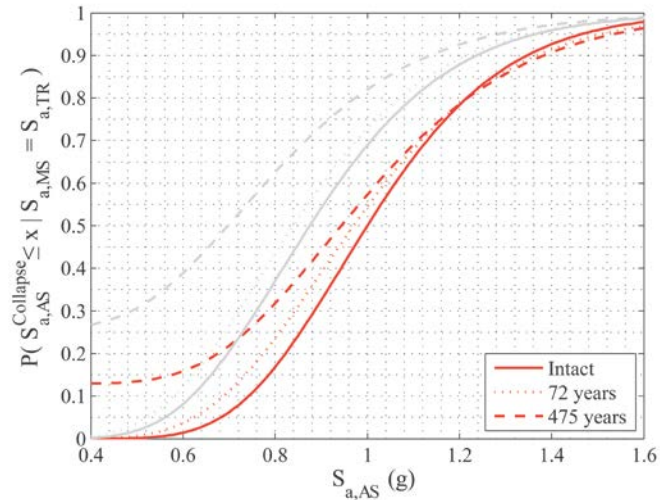


Fig. 6 – T_R -dependent fragility curves and fragility curve for model wrap1.

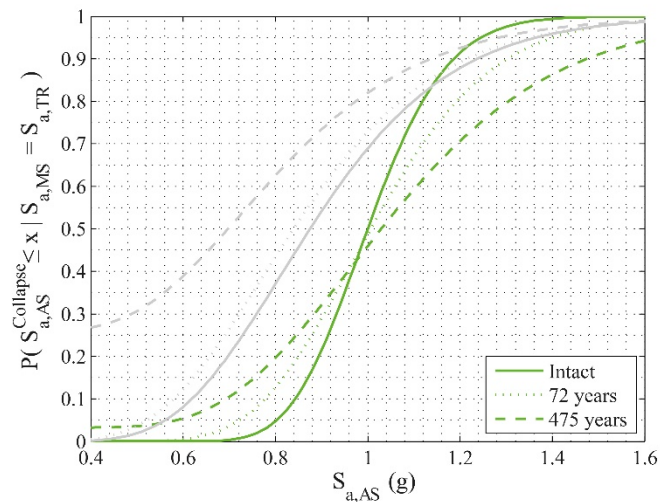


Fig. 7 – T_R -dependent fragility curves and fragility curve for model wrap2.

In particular, for $T_R=475$ yrs a slight increase in median aftershock capacity, respect to the MS capacity, can be noted. This kind of effect was previous noted in [28, 29], and it could be explained considering the possibility of accumulation of damage through the building. In fact, while for the non-ductile building the ductility and, thus, the possibility of damage accumulation is limited by brittle failures, for the *wrap2* model a higher level of damage can be achieved before the collapse occurs. In particular, residual drifts for the model *wrap2* can be higher due to the possibility for the building to experience significant damage before collapse. In this case, it may become noticeable the polarity of the MS-AS ground motion sequence (i.e., the directions of the AS and MS) in the determination of REC: depending on earthquake polarity, MS and AS may be applied in the same direction (tending to increase residual drifts) or in opposite directions (reducing residual drifts), tending to reduce or to increase the REC, respectively. Further, the higher damage experienced during earthquakes may significantly reduce building lateral strength with a consequent reduction of seismic demand. However, further analyses are necessary for a better comprehension of this phenomenon. It can also be noted that the dispersion of AS-fragilities increases as T_R increases. This can be explained considering that the level damage experienced for higher return periods shows a high scatter consequently leading to a different REC.



Finally, it can be noted that despite the effectiveness of more diffuse column wrapping is limited when considering collapse capacity for the intact building, the difference in retrofit scheme may significantly modify building structural performances with respect to future earthquakes.

5.3 Economic Losses

The framework outlined in §3 was adopted to calculate economic losses for the case-study building. Having simulated the response of the building for different intensities corresponding to return periods of 72 and 2475 yrs, the loss analysis was performed using the fragility data and costs as indicated in [16]. In particular, to solve PEER equation integral, a Monte Carlo procedure was adopted to generate additional response parameters (EDP), see [18, 19]. In this study, 1000 realizations were performed for each intensity level to obtain stable cost estimates. For each realization and PG, a unique damage state was determined using a uniform random generator over the interval [0,1] considering the probability of the PG experiencing each damage state at the EDP obtained from structural analysis. Once the damage state for a performance group is identified, the repair action and the associate repair cost for that performance group is obtained by multiplying cost of new elements by corresponding normalized repair costs by the number of elements in the considered PG. If collapse has not occurred, losses are calculated for each realization based on the damage sustained by each component and the consequence functions assigned to each performance group and by summing repair costs of each PG. If structural collapse was detected, the total repair cost is calculated using the replacement value of the building plus additional costs related to demolition and debris removal (15% of the replacement value of the building). When CFRP wrapping is applied, the additional cost due to retrofit intervention is accounted as a repair cost determining a shift to the right of the normalized cost curve. Next, direct economic losses are expressed in terms of normalized repair costs (c_r), that are obtained dividing repair costs by the building's replacement value. The probability of exceeding a certain level of total normalized repair cost accounting for both the collapse and non-collapse cases can be calculated as:

$$P(C_r \geq x) = P(C_r \geq x | IM, NC)[1 - P(C | IM)] + P(C_r \geq x | IM, C)P(C | IM) \quad (3)$$

where $P(C_r \geq x | IM, NC)$ is the probability conditioned on IM when the structure do not collapses that the normalized repair cost exceeds x ; $P(C_r \geq x | IM, C)$ is the probability of exceeding the normalized repair cost x given the collapse, that is actually independent from IM and equal to the replacement value of the building; $P(C | IM)$ is the probability of collapse conditioned on IM.

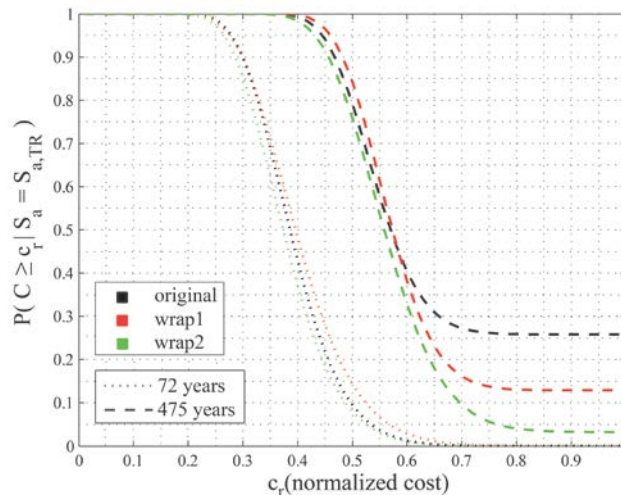


Fig. 8 – Probability of exceeding normalized cost at five different hazard levels.

The complementary cumulative distribution of the total normalized repair costs, is shown in Fig. 8 considering two different hazard levels. Results for different models are reported with different colors. Fig. 8 shows that; with the increase of the damaging action (i.e., return period) the repair cost inflates making the curve translate rightward.



Furthermore, it can be noted that total repair cost of at least 20-25% can be expected even for the lowest considered return period. This high cost is due to the nonstructural components and contents, which significantly contribute to damage and costs even for relatively low levels of seismic action. It is worth to note that the total normalized repair cost conditioned on the return period of the damaging action at the site is strongly influenced by occurred collapse cases, see second member of the Eq.(3). This effect is particularly evident for higher return periods, for which the curve results translated upward.

It is interesting to note that, despite the collapse capacities for the models *wrap1* and *wrap2* significantly increase with respect to the original building, a similar beneficial effect is not obtained in terms of repair costs. In fact, CFRP wrapping does not influence building linear response in a significant way, and thus very small variations in building response are expected when the seismic demand is relatively low. In particular, for 72yrs, the costs of wrapping, summed to repair costs, leads to an increase of total costs for *wrap1*, with respect to the original building. For *wrap2* scheme, a reduction of repair costs can be evidenced, although it is not substantial. However, similar considerations can be carried out for $T_R=475$ yrs, where the effect of retrofit on repair costs does not significantly vary with respect to cost for the original building, except for the probability of reaching a unit normalized repair cost. In fact, for the original model there is a probability of about 30% that the normalized repair cost is equal to substitution cost, while due to the effect of wrapping schemes *wrap1* and *wrap2* on collapse capacity, this probability drops to 12% and 3.2%, respectively. The small sensitivity of median repair costs to the retrofit strategies relies on the peculiar effect of CFRP wrapping, which increases lateral displacement capacity avoiding brittle failures. In particular, the adopted schemes do not significantly affect the repair costs of nonstructural building components, which represent the main part of repair costs.

6. Conclusions

The study presented in this paper analyzes, with a detailed case study, the advantages related to the application of structural retrofit prior of damaging earthquake events, to support reparability decisions in the perspective of a performance-based framework. Both the residual capacity variation, that is connected to the variation of safety, and direct economic losses are considered as significant metrics for reparability decisions.

The response of an existing non-ductile RC frame is simulated using a refined 2D finite element model that properly accounts for possible brittle failures of structural members and captures typical non-ductile RC frames failure modes. Two different retrofit schemes adopting complete full-height CFRP wrapping are considered to study the effectiveness of the mitigation strategies. Both Residual Capacity (REC), expressed in probabilistic terms by means of aftershock fragility curves, and normalized repair costs were computed with reference to two different earthquake scenarios considered for the Los Angeles area. The future seismic performances of retrofitted structures before damage are compared with the case in which no mitigation strategies have been adopted, showing the advantages and the effectiveness of different categories of intervention for different earthquake scenarios.

Results for the intact building show that the application of wrapping scheme only applied to 1st and 7th storeys (*wrap1*) is effective in increasing collapse capacity. In particular, the median collapse capacity increases of about 14% with respect to the original building. The adoption of a widespread wrapping scheme (*wrap2*), including 1st and 4th to 7th storeys, does not influence median intact capacity, despite leading to a dispersion reduction. This effect can be explained considering that the most of collapses for *wrap1* occurs at 1st storey, and for those cases, additional wrappings considered in scheme *wrap2* are ineffective to prevent the most of collapses, consequently leading to the same median collapse capacity.

The results from MS-AS analyses show that for the non-ductile building the REC of a MS-damaged non-ductile building may be significantly smaller than that of an intact building. However, when *wrap1* scheme is considered, a smaller reduction of REC can be found for same return period due to the increment of displacement ductility associated with retrofit scheme. For retrofit scheme *wrap2*, the beneficial effect is more evident: in particular, while for smaller return period the median REC does not vary with respect to the capacity of the intact building, for the 475yrs return period also an increase of median REC is attained. This may be ascribed to the possibility for the structure of experiencing larger deformation and a reduction of seismic demand due to the period elongation. However, further investigations are required to properly comprehend this phenomenon.



Adopting existing component fragilities and repair costs, direct economic losses were computed for the case study building. The results show that repair costs for the non-ductile building can be significant also for low return periods due to the damage of nonstructural components and contents, with a total repair cost of at least 20-25% for $T_R=72$ yrs. For increasing T_R , the contribution of collapse cases becomes more significant, leading to increasing probability of overcoming the reconstruction costs. The effectiveness of CFRP wrapping schemes in terms of repair and retrofit costs is much reduced because the retrofit scheme only increases global ductility of the building, while does not substantially influence experienced drifts and acceleration. Particularly, the *wrap1* scheme leads to an increase of total costs due to the incidence of retrofit costs and only for $T_R=475$ years the effectiveness of two retrofit schemes becomes significant, leading to the reduction of the probability of having repair cost equal to the cost of reconstruction.

The present study shows that, as expected, the adoption of retrofit strategies increasing ductility capacity does not significantly vary repair costs, except the portion depending on costs related to collapse. However, the effectiveness of this strategy is demonstrated both in terms of collapse capacity and in terms of reduction of REC loss, that for non-ductile buildings may influence building reparability after damage. Further studies are required to assess the advantages of other alternative strategies in terms of seismic performances, especially when applied to a larger building inventory. Moreover, indirect losses, that may be particularly significant for communities following strong earthquakes, should be explicitly considered in future works.

7. Acknowledgements

This study was performed within the framework of the PON METROPOLIS “Metodologie e tecnologie integrate e sostenibili per l'adattamento e la sicurezza di sistemi urbani” grant n. PON03PE_00093_4 and the joint program DPC-Reluis 2014-2018 Task 3.3: “Reparability limit state and damage cumulated effects”. The S.Co.P.E. computing infrastructure at the University of Naples Federico II was used for parallel computing.

8. References

- [1] NIST, G. GCR 10-917-7 (ATC-76-5) (2010). Program plan for the development of collapse assessment and mitigation strategies for existing reinforced concrete buildings. *National Institute of Standards and Technology*, Washington, DC.
- [2] FEMA 454 (2006). Designing for Earthquakes: A Manual for Architects, Federal Emergency Management Agency. U.S. Department of Homeland Security, Washington, DC.
- [3] Gaetani d'Aragona M, Polese M, Elwood KJ, Shoraka MB, Prota A, & Manfredi G (2015). Building Performance Loss after Damaging Earthquakes: an Investigation Towards Reparability Decisions. In *12th International Conference on Applications of Statistics and Probability in Civil Engineering* (pp. 258-1).
- [4] Polese M, Di Ludovico M, Prota A, Manfredi G (2012). Damage-dependent vulnerability curves for existing buildings. *Earthquake Engng Struct. Dyn.*, 42 (6), 853-870, DOI: 10.1002/eqe.2249.
- [5] Pacific Earthquake Engineering Research Center (PEER). PEER NGA database flatfile (2010). <<http://peer.berkeley.edu/nga/flatfile.html>> [10 September 2010].
- [6] Baradaran Shoraka M, Yang TY, Elwood KJ, (2013). Seismic Loss estimation of non-ductile reinforced concrete buildings, *Earthquake Engineering and Structural Dynamics*; 42, 297-310.
- [7] Elwood KJ, Holmes WT, Comartin D, Heintz C, Rojahn C, Dragovich J, McCabe S, Mahoney M (2012). Collapse Assessment and Mitigation of Nonductile Concrete Buildings: ATC-76-5/ATC-78/ATC-95. *15thWCEE*, Lisbon, Portugal, 24–28 Sept.
- [8] Vamvatsikos D, & Cornell CA (2002). Incremental dynamic analysis. *Earthquake Engineering & Structural Dynamics*; 31(3), 491-514.
- [9] Benjamin JR, Cornell CA. (1970). Probability, statistics and decision for civil engineers, McGraw-Hill.
- [10] Ebrahimian H, Jalayer F, Asprone D, Lombardi AM, Marzocchi W, Prota A, Manfredi G. (2014). A Performance-based Framework for Adaptive Seismic Aftershock Risk Assessment. *Earthquake Engng Struct. Dyn.*, 43(14): 2179–2197.



- [11] Jalayer, F., Asprone, D., Prota, A., Manfredi, G. (2011). A decision support system for post-earthquake reliability assessment of structures subjected to after-shocks: an application to L'Aquila earthquake, 2009. *Bull Earthquake Eng*, 9 (4): 997-1014.
- [12] Jalayer F, Beck JL, Zareian F (2012). Intensity Measures of Ground Shaking Based on Information Theory. *Journal of Engineering Mechanics*, 138 (3): 307-316.
- [13] Porter KA (2003). An overview of PEER's performance-based earthquake engineering methodology. Proceedings of Ninth International Conference on Applications of Statistics and Probability in Civil Engineering, San Francisco, CA.
- [14] Ramirez CM, & Miranda E (2009). Building-specific loss estimation methods & tools for simplified performance-based earthquake engineering, PhD dissertation; Stanford University.
- [15] Aslani H, Miranda E (2005). Probabilistic Earthquake Loss Estimation and Loss Disaggregation in Building. Technical Report No. 157, John A. Blume Center Earthquake Engineering Center, Stanford, CA.
- [16] Gaetani d'Aragona M, Polese M., Prota A (2015). Relationship between the Variation of Seismic Capacity after Damaging Earthquakes, Collapse Probability and Repair Costs: Detailed Evaluation for a Non-Ductile Building. *COMPdyn 5th ECCOMAS Thematic Conference on Computational Methods in Structural Dynamics and Earthquake Engineering* May 25-27, 2015 Crete Island, Greece.
- [17] Gaetani d'Aragona M. Post-Earthquake Assessment of Damaged non-Ductile Buildings: Detailed Evaluation for Rational Reparability Decisions, Ph.D. Dissertation, University of Naples Federico II, Italy, 2015.
- [18] FEMA P-58 (2012). Next-generation Seismic Performance Assessment for Buildings, Volume 1 – Methodology, Federal Emergency Management Agency, Washington, D.C.
- [19] Yang TY, Moehle J, Stojadinovic B, Der Kiureghian A (2009). Seismic performance evaluation of facilities: Methodology and implementation. *Journal of Structural Engineering*; 135(10): 1146–1154.
- [20] McKenna F, Fenves GL, Scott MH, and Jeremic B (2000). Open System for Earthquake Engineering Simulation (OpenSees). *Pacific Earthquake Engineering Research Center*, University of California, Berkeley, CA, 2000.
- [21] de Souza RM (2000). Force-based finite element for large displacement inelastic analysis of frames. PhD Dissertation, University of California, Berkeley, USA, California.
- [22] Alath S, Kunnath SK. Modeling inelastic shear deformation in RC beam-column joints. *Engineering Mechanics Proceedings of 10th Conference*, May 21-24, ASCE, Boulder, CO, USA, 1995; 822–825.
- [23] Elwood KJ. Modelling Failures in Existing Reinforced Concrete Columns. *Canadian Journal of Civil Engineering*, 2004: 846-859.
- [24] Celik OC, and Ellingwood BR (2008). Modeling beam-column joints in fragility assessment of gravity load designed reinforced concrete frames. *Journal of Earthquake Engineering*; 12(3), 357-381.
- [25] ACI 369R-11 (2011). Guide for Seismic Rehabilitation of Existing Concrete Frame Buildings and Commentary. Report by ACI committee 369, *American Concrete Institute*. ISBN: 978-0-87031-419-3
- [26] ACI 440.2R-08 (2008). Guide for the design and construction of externally bonded FRP systems for strengthening concrete structures. Report by ACI Committee 440.2R-08. Farmington Hills, MI, USA: *American Concrete Institute*.
- [27] Spoelstra MR, & Monti G (1999). FRP-confined concrete model. *Journal of composites for construction*, 3(3), 143-150.
- [28] Polese M, Gaetani d'Aragona MG, Prota A, & Manfredi G (2013). Seismic Behavior of Damaged Buildings: a Comparison of Static and Dynamic Nonlinear Approach. *COMPdyn 4th ECCOMAS Thematic Conference on Computational Methods in Structural Dynamics and Earthquake Engineering*. June 12-14, Kos Island, Greece.
- [29] Raghunandan M, Liel AB, & Luco N. (2015). Aftershock collapse vulnerability assessment of reinforced concrete frame structures. *Earthquake Engineering & Structural Dynamics*, 44(3), 419-439.